Investigating Displacement Sensitivity of a Michelson Interferometer

Raisa Tasnim Raofa
Department of Physics, The College of Wooster, Wooster, Ohio 44691, USA
(Dated: May 21, 2022)

Kenneth G. Libbrecht and his team from Caltech were successful in demonstrating picometer sensitivity using a basic Michelson interferometer. In this experiment, we attempted to recreate the phenomena by using a classical Michelson interferometer and a photodetector. We were successful in observing the change in output intensity on the screen due to displacement of one of the mirrors However, we were unable to measure the numerical value of this intensity.

I. INTRODUCTION

Optical interferometry is a method of measuring distance changes with a precision down to sub nanometer scale using lasers and other optical devices, such as mirror, beamsplitter, etc. [1]

Some of the well-known optical interferometer are Michelson Interferometer, Fabry-Perot Interferometer, Fizeau-Laurent surface intereferometer, etc. [2] Among them, Michelson interferometer is a fairly basic optical system constructed by the American physicist A. A. Michelson in 1881. The setup consists of a half-silvered mirror (beamsplitter) and two mirrors where one of them is movable. [3]

Despite the simplicity of the Michelson interferometer and its modifications, they are used extensively in the optical industry for testing lenses and prisms, for measuring index of refraction, and for examining minute details of surfaces. [2]

II. THEORY

A. Interference

According to Demtröder [4], we can observe interference of light using the Young's double slit experiment. In this experiment, when both of the slits are open, the observed intensity does not equal the sum $I_1 + I_2$, but an interference pattern similar to that of in Fig. 1 appears on the screen and it can be described by

$$\begin{aligned} I(x) &= |A_1(x) + A_2(x)|^2 \\ &= I_1 + I_2 + 2A_1A_2\cos(\Delta\phi(x)), \end{aligned} \tag{1}$$

where A_i is the amplitude of the partial wave transmitted through the slit S_i and $\delta\phi = (2\pi/\lambda)\Delta s$ is the phase difference between the two interfering partial waves at the point $P(y)$ on the photoplate, resulting from the path difference

$$\Delta s(y) = \overline{S_1P(y)} - \overline{S_2P(y)}. \tag{2}$$

There are two different kinds of interference which are constructive interference and destructive interference.

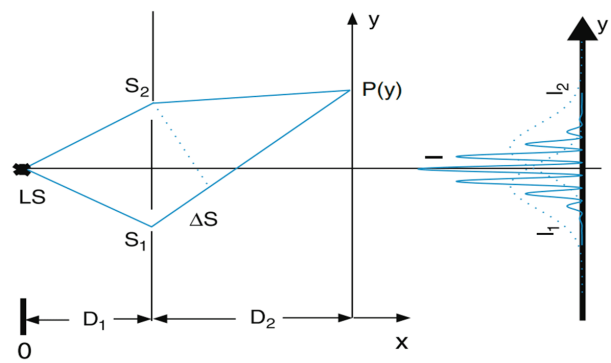

FIG. 1: Young's double slit experiment with photons where LS is the laser source, S_1 and S_2 are the distance of the slits from the laser. ΔS is the distance between S_1 and S_2. I is the intensity of the maximum bright fringe, wheres I_1 is the intensity of the projected laser beam on the screen if I_2 was covered and the I_2 is when the opposite happens (from [4]).

.

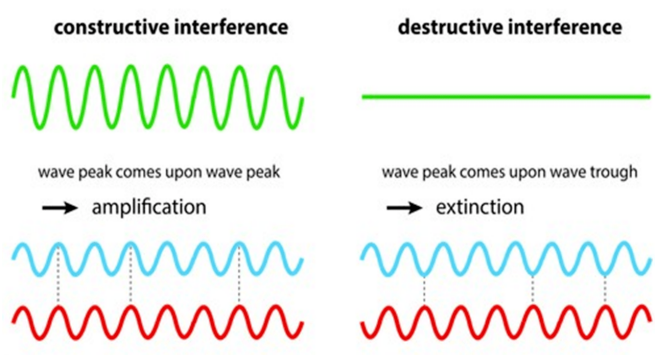

FIG. 2: Example of constructive and destructive interference of two waves (from [5]).

.

Constructive interference happens when the beams are in phase (partially or completely) and the light waves add and the full initial laser intensity incidents at the screen. But, if the light waves are out of phase, then the resultant intensity is 0. Therefore, there will be no output intensity on the screen of the interferometer. As a result, we can see constructive and destructive interferences of light beams as shown in Fig. 2.

1.png

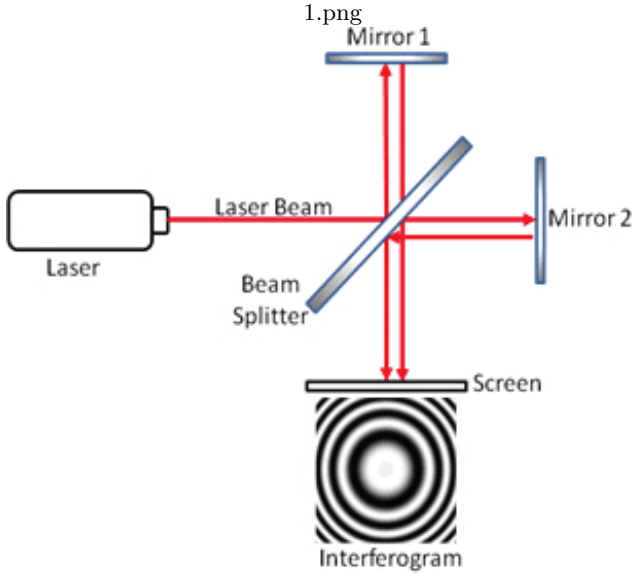

FIG. 3: Schematic figure of Michelson interferometer where we can see different interference pattern on the screen (from [6]).

.

B. Michelson Interferometer

Interferometers are based on the interference of two or more coherent partial waves. One of the experimental realization of the two-beam interference is the Michelson interferometer. From the schematic diagram of the interferometer in Fig. 3 we can see that the incoming parallel beam is split by a beam splitter into two partial beams, which are reflected by the mirrors Mirror 1 and Mirror 2 and are again superimposed at the beamsplitter before they are projected on the screen in Fig. 3. If Mirror 2 is translated by Δx, the path difference between the two interfering beams changes by $\Delta s = 2\Delta x$.

If the position x of the translating mirror (Mirror 2 in Fig. 3) is varied over a small distance, then the detector voltage V_{det} is

$$V_{\text{det}} = V_{\text{min}} + \frac{1}{2}(V_{\text{max}} - V_{\text{min}})[1 + \cos 2kx], \qquad (3)$$

where V_{max} and V_{min} are the maximum and minimum voltages respectively, and $k = 2\pi/\lambda$ is the wavenumber of the laser.

The interferometer fringe (A fringe is a bright or dark band caused by beams of light that are in phase or out of phase with one another. [7]) is

$$F_{\text{C}} = \frac{V_{\text{max}} - V_{\text{min}}}{V_{\text{max}} + V_{\text{min}}}. \qquad (4)$$

A high fringe contrast with $F_{\text{C}} \approx 1$ is desirable for obtaining the best interferometer sensitivity. [8]

.png

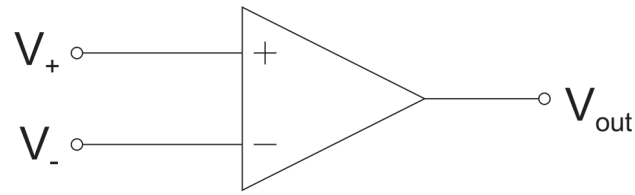

FIG. 4: Signal connections in an op-amp (from [10])

.

C. Operational Amplifiers (Op-Amp)

Op-amp, a differential amplifier, is an example of integrated circuits which consists of many individual circuit elements, such as transistors and resistors, fabricated and interconnected on a single "chip" of silicon. Negative feedback is a characteristic of op-amps which promotes stability of the circuit and makes the circuit performance less dependent on component imperfections, such as temperature, engineering tolerance, etc. [9]

A differential amplifier takes the difference of two inputs, V_+ and V_-, and amplifies it by an amount G that is called the *open-loop* gain. The output Voltage is

$$V_{\text{out}} = G(V_+ - V_-). \qquad (5)$$

However, G is not a reliable parameter as it depends on the frequency and we may not have any control over it. Retrospectively, with negative feedback, we can design a circuit with a gain that is constant and that we can control. We can do so by feeding the *inverting* input V_- with a sample of the output.

If we connect an input voltage V_+ to the *noninverting* input of the op-amp (V_+), and a fraction $1/A$ of the output to the inverting input V_-, as shown in Fig. 4. Then Eq. (5) becomes,

$$\begin{aligned} V_{\text{out}} &= G(V_{\text{in}} - \frac{1}{A}V_{\text{out}}) \\ V_{\text{out}} &= \frac{G}{1 + \frac{1}{A}}V_{\text{in}}, \end{aligned} \qquad (6)$$

where A is the gain of the circuit.

If $G \gg A$, then there is a negative feedback in the circuit as shown in Fig. 5.

Eq. (6) states that the output voltage is equal to the input voltage multiplied by a gain A. [10]

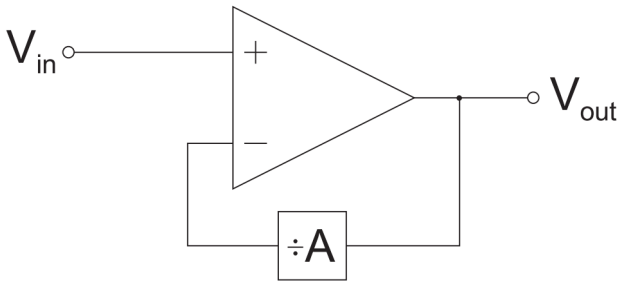

FIG. 5: Negative feedback with an op-amp (from [10])

.

D. Photodiode

Photodiodes are doped semiconductor radiation detectors that can be used either as photoconductive or as photovoltaic devices. When the semiconductor diode is irradiated, electrons are excited from valence into the conduction band. This produces free charge carriers and increases the conductivity of the diode. [4]

In the non-illuminated p-n junction of the diode, the diffusion of the electrons from the n-region into the p-region and of the holes into the opposite direction produces a charge separation and therefore a diffusion voltage V_{D} across the junction. This diffusion voltage cannot be detected by an external voltmeter because it is just compensated by the opposite contact potentials between the connections to the voltmeter and the n- or p-part at both end faces of the diode.

If the p-n junction is illuminated, electron-hole pairs are creates by photon absorption. The electrons are driven by the diffusion voltage into the n-region and the holes into the p-region. This leads to a decrease ΔV_D of the diffusion voltage, which appears as the photovoltage,

$$V_{\mathrm{photo}} = \Delta V_{\mathrm{D}}, \tag{7}$$

across the open electrodes of the diode. [4]

E. Piezoelectric Actuator

Piezoelectricity is an electromechanical phenomenon that involves interaction between the mechanical (elastic) and the electrical behaviour of a material. A typical piezoelectric material produces an electric charge or voltage in response to a mechanical stress, and vice versa. The former is known as the direct piezoelectric phenomenon, while the latter is known as the converse piezoelectric phenomenon. The direct and converse effects of commercial piezoelectric materials are achieved by a so-called poling process, which involves exposing the material to high temperatures while imposing high

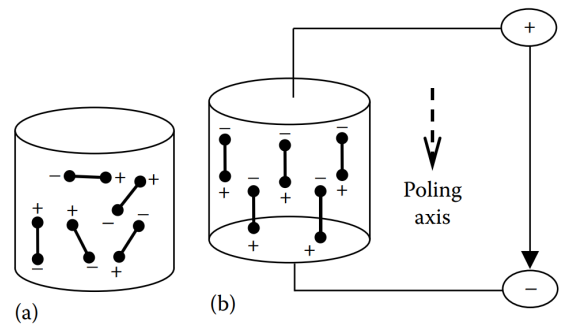

FIG. 6: The micromechanism of the piezoelectric effect. (a) No voltage and (b) poling (from [11])

.

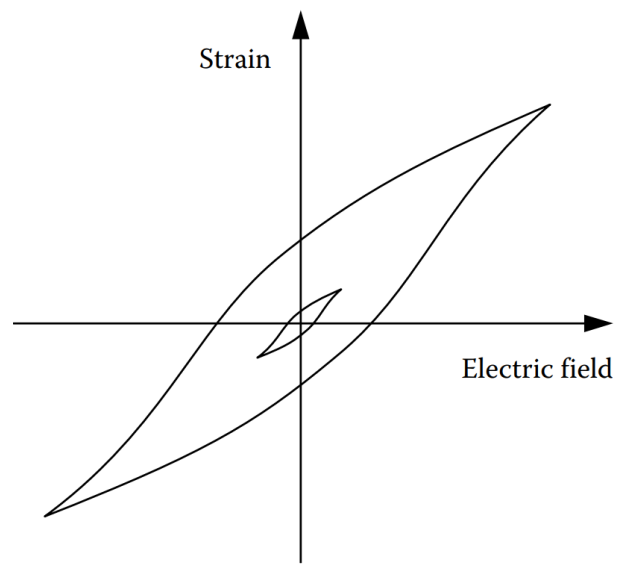

FIG. 7: Field–strain relation of a typical piezoelectric material (From [11])

.

electric field intensity in a desired direction. Before the poling process, the piezoelectric material exhibits no piezoelectric properties, and it is isotropic because of the random orientation of the dipoles, as shown in Fig. 6. Then, a driving voltage with a certain direction of polarity causes the cylinder to deform.

Macroscopically, piezoelectric materials exhibit field–strain relation, as shown in Fig. 7. The relation is nearly linear for low electric fields, which provides advantage for system modeling and control realization. But, that is not the case at high electric field, and domains expand and switch. Therefore, it can be detrimental to employ piezoelectric material in control implementation associated with high electric field. [11]

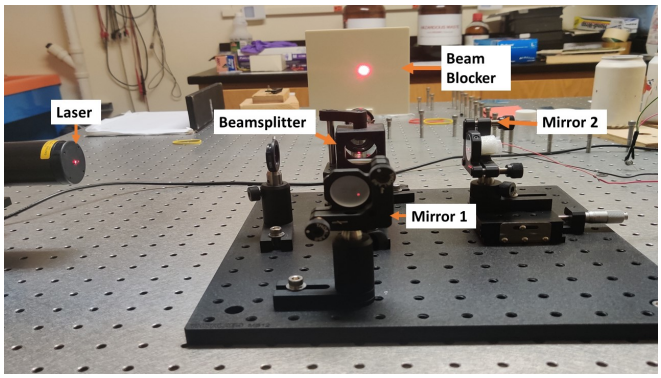

FIG. 8: The optical layout of Michelson Interferometer used for our experiment.

III. SET-UP

A. The Michelson Interferometer

We use Newport Integrity 1 VCS Optical Table System in order to reduce noise in the interferometer signal arising from benchtop vibrations. This system is adequate as long as the table is not unnecessarily perturbed. Most of our optical devices except for the laser is mounted on a 12.7 mm thick aluminium breadboard (Thorlabs MB 12) on the Optical Table System in order to help mobility if need arises.

We use a helium-neon laser (IEC825 - 1:1993) which produces a 4.58 mW polarized 632.8 nm beam. The beamsplitter (Thorlabs BS013) is a cube with 1 inch dimensions. The splitter coating has a 50 : 50 split ratio and all the surfaces have a $400 - 700$nm BBAR coating. The dielectric beamsplitter coating applied to the hypotenuse gives roughly equal transmitted and reflected beams. Mirrors 1 and 2 (both Thorlabs BB1-E02) are mounted using standard optical mounts. These mounts play a significant part in reducing any unwanted motions of the optical elements.

We glued the piezoelectric stack transducer (PZT) (Steminc SMPAK155510D10) to our movable mirror (Mirror 2 in Fig. 8).

Upon successful completion of building a Michelson interferometer, we get an interferometer like that of in Fig.‘8.

The photodetector includes a Silicon photodiode (OSRAM SFH 221) with a 1.54 mm^2 active area and some amplifying electronics as shown in Fig. 9 to convert the incident optical power to the detector voltage, V_{det}. We will talk about the circuit in details in Section III B.

diagram.jpg

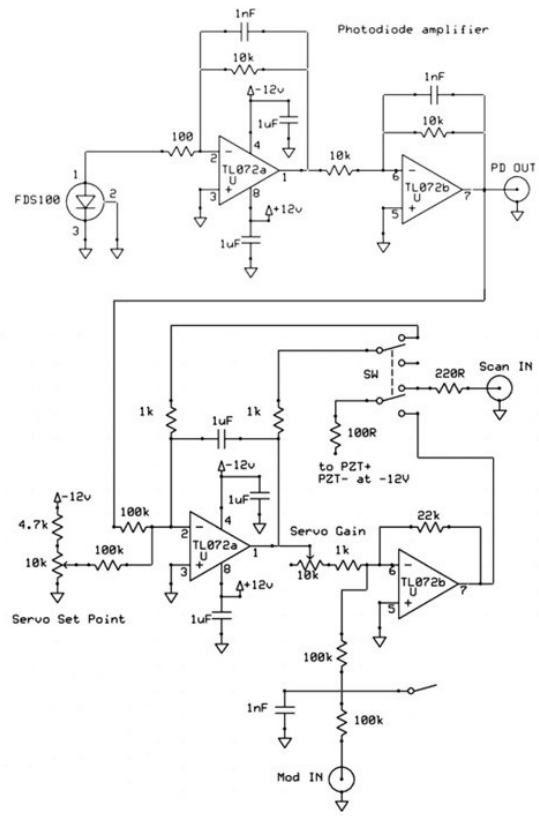

FIG. 9: The electronics used to scan, lock, and modulate the interferometer signal. With switch SW in the SCAN position, a signal input to the Scan IN port is sent essentially directly to the PZT. With the switch in the LOCK position, a feedback loop locks the mirror/PZT so the average photodiode signal (PD Out) equals the Servo Set Point. With the interferometer locked, a signal sent to the Mod IN port additionally modulates the mirror position (from [8])

.

B. The Circuit

In order to convert our output laser beam to voltage, we built a circuit which has a diagram as shown in Fig. 9. The circuit consists of four op-amps, and multiple resistors, and capacitors of different values as we can see in Fig. 10. In order to ensure that all the op-amps in our circuit are working properly, we tested the output of all the op-amps using a Function Generator and Oscilloscope. The final set-up used for testing the output voltage of the op-amps was as shown in Fig. 11 Fig. 12 shows us the sinusoidal waves of the output voltage of all the four op-amps used in the circuit.

Eventually, we added two potentiometers, and a Double-Pole Double-Throw (DPDT) switch used in the electronics in order to find the numerical values of the detected voltage from the output light intensity and ensure the signal input is sent to the PZT as shown in Fig. 10.

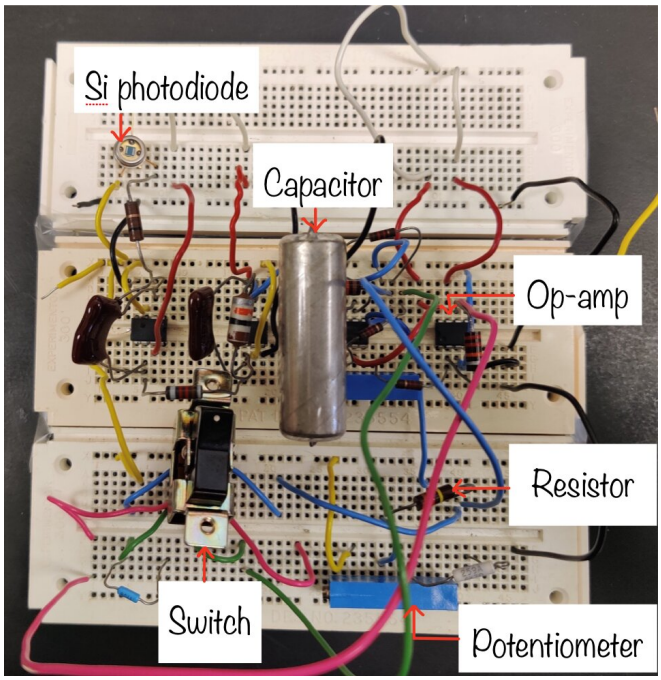

FIG. 10: Top view of the electronics which converts light intensity into voltage using the photodiode added in the circuit.

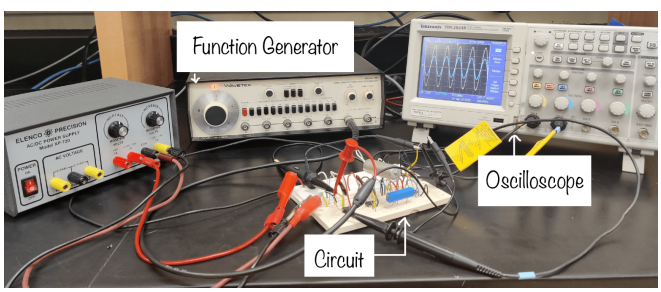

FIG. 11: Experimental set-up used in order to investigate the output signals of all the four op-amps used in the circuit.

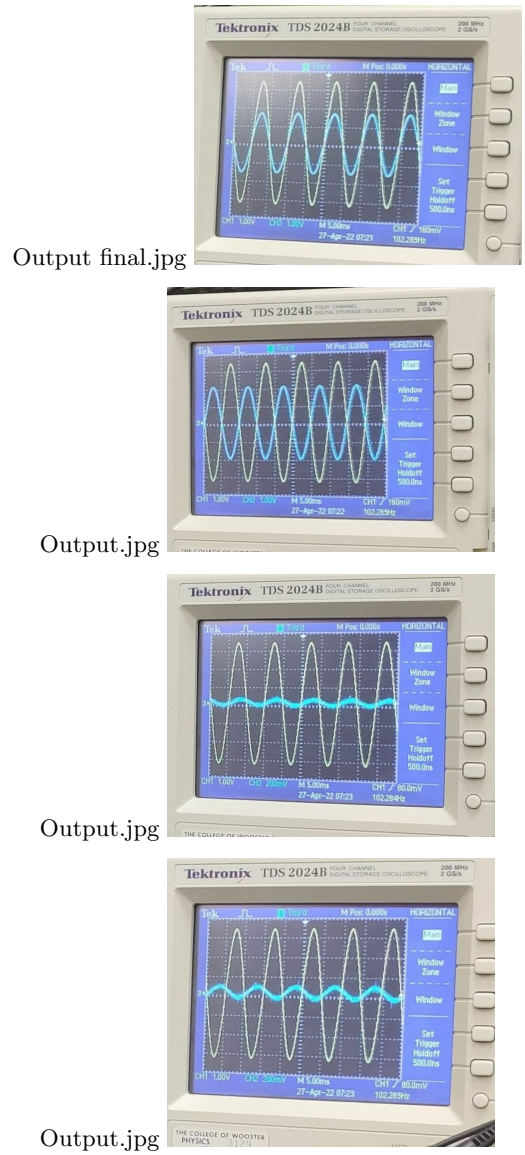

FIG. 12: Output signals (Blue wave in the Oscilloscope) of the first, second, third and fourth op-amps used in the circuit compared to that of the input signal (Yellow wave in the Oscilloscope) are shown from top to bottom (where the top most one is the first op-amp and the bottom most one is the fourth op-amp of the circuit). We used a function generator in order to test the response of circuit in order to determine the output voltage of each of the op-amp compared to that of the input voltage. In real life electronics, this is a very handy way to ensure that all your op-amps are functioning properly.

IV. OBSERVATION

A satisfactory alignment of the interferometer is straightforward and easy to achieve, but doing so requires an understanding of how real-world optics can differ from the idealized case that is often presented. In the Michelson interferometer, at the ends of the interferometer arms yields a recombined beam that is sent directly back toward the laser. This beam typically reflects off the front mirror of the laser and reenters the interferometer, yielding an optical cacophony of multiple reflections and unwanted interference effects. In order to solve this problem, we needed to slightly misalign(or tilt) the movable mirror (M2 in Fig. 13).

Due to the lack of time, we were unable to numerically calculate the V_{det}. But, we observed that displacing Mirror 2 of our interferometer did not change the number of fringes that we see on the beam blocker as shown in Fig. 8. However, it changed how clearly we can see the fringes. In other words, there was a change in the intensity due to the change in distance between the beamsplitter and Mirror 2 caused a change in the output intensity.

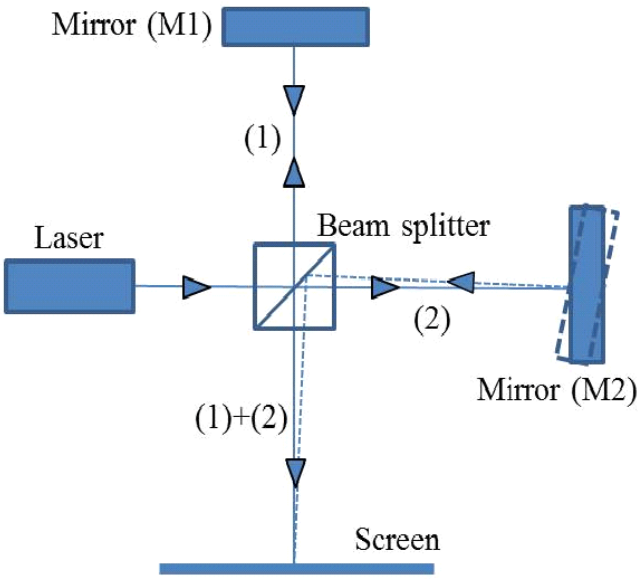

FIG. 13: Schematic Diagram of Michelson Interferometer after tilting M2 (from [10]).

V. CONCLUSION

We were unable to confirm how small of a change in displacement we can measure using a basic Michelson interferometer. But, we were able to successfully observe the effects of displacement of a mirror using a Michelson interferometer.

VI. ACKNOWLEDGMENT

I thank Dr. Niklas Manz for providing help and valuable advice during the whole duration. Additionally, I thank Dr. Robin Bjorkquist, and Dr. Cody Leary for their guidance in building the circuit and interferometer respectively. This Jr. I.S. project was supported by the Koontz Fund.

[1] Wiora, G., Weber, M. & Chanbai, S. *Optical Interferometry*, 2483–2488 (Springer US, Boston, MA, 2013). URL `https://doi.org/10.1007/978-0-387-92897-5_317`.

[2] Optical Interferometer. `https://www.britannica.com/technology/optical-interferometer`. Accessed on 2022 April 08.

[3] Michelson, A. A. & Morley, E. W. On the Relative Motion of the Earth and the Luminiferous Ether. *American Journal of Science* **s3-34**, 333–345 (1887). URL `https://www.ajsonline.org/content/s3-34/203/333`. https://www.ajsonline.org/content/s3-34/203/333.full.pdf.

[4] Demtröder, W. *Atoms, molecules and photons: An introduction to atomic-, molecular- and quantum-physics* (Springer Verlag, 2006).

[5] What are binaural beats? `https://www.scienceabc.com/pure-sciences/what-are-binaural-beats.html` (2022).

[6] Schematic Figure of Michelson Interferometer. `https://www.researchgate.net/figure/Schematic-figure-of-Michelson-interferometer_fig1_306050242` (2022).

[7] Interference Fringe. `https://www.britannica.com/science/interference-fringe`. Accessed on 2022 May 06.

[8] Libbrecht, K. G. & Black, E. D. A Basic Michelson Laser Interferometer for the Undergraduate Teaching Laboratory Demonstrating Picometer Sensitivity. *American Journal of Physics* **83**, 409–417 (2015).

[9] Horowitz, P. & Hill, W. *The Art of Electronics* (Cambridge University Press, 2015).

[10] Galvez, E. *Electronics with Discrete Components*. Electronics with Discrete Components (Wiley, 2012). URL `https://books.google.com/books?id=AmtSFd66z9MC`.

[11] Choi, S. & Han, Y. *Piezoelectric Actuators: Control Applications of Smart Materials* (CRC Press, 2016). URL `https://books.google.com/books?id=iKSoTKpgFpUC`.